BIOCHEMISTRY
including biophysical chemistry & molecular biology
Article

Biochemistry **2010,** *49,* 761–771 761
DOI: 10.1021/bi901846y

Identification of the Binding Site for the Regulatory Calcium-Binding Domain in the Catalytic Domain of NOX5[†]

Fabiana Tirone,*[,‡] Laura Radu,[§,∥] Constantin T. Craescu,[§,∥,⊥] and Jos A. Cox*[,‡]

[‡]*Departement of Biochemistry, University of Geneva, Geneva 4, Switzerland,* [§]*INSERM U759, and* [∥]*Institut Curie, Centre Universitaire Paris-Sud, 91405 Orsay Cedex, France* [⊥]*Deceased*

Received October 28, 2009; Revised Manuscript Received December 15, 2009

ABSTRACT: NADPH oxidases (NOX) are important superoxide producing enzymes that regulate a variety of physiological and pathological processes such as bacteria killing, angiogenesis, sperm−oocyte fusion, and oxygen sensing. NOX5 is a member of the NOX family but distinct from the others by the fact that it contains a long N-terminus with four EF-hand Ca^{2+}-binding sites (NOX5-EF). NOX5 generates superoxide in response to intracellular Ca^{2+} elevation *in vivo* and in a cell-free system. Previously, we have shown that the regulatory N-terminal EF-hand domain interacts directly and in a Ca^{2+}-dependent manner with the catalytic C-terminal catalytic dehydrogenase domain (CDHD) of the enzyme, leading to its activation. Here we have characterized the interaction site for the regulatory NOX5-EF in the catalytic CDHD of NOX5 using cloned fragments and synthetic peptides of the CDHD. The interaction was monitored with pull-down techniques, cross-linking experiments, tryptophan fluorescence, hydrophobic exposure, isothermal titration calorimetry, and cell-free system enzymatic assays. This site is composed of two short segments: the 637−660 segment, referred to as the regulatory EF-hand-binding domain (REFBD), and the 489−505 segment, previously identified as the phosphorylation region (PhosR). NOX5-EF binds to these two segments in a Ca^{2+}-dependent way, and the superoxide generation by NOX5 depends on this interaction. Controlled proteolysis suggests that the REFBD is autoinhibitory and inhibition is relieved by NOX5-EF.

In humans reactive oxygen species are generated by five NADPH[1] oxidase (NOX1−5) isoforms, which differ importantly in the way their activity is regulated. NOX1, NOX2 (the best known phagocytic NOX), and NOX3 interact with several regulatory subunits, NOX4 seems constitutively active, and NOX5 is regulated by Ca^{2+} (reviewed in refs *1*−*4*). NOX5 possesses a domain with four functional EF-hands (NOX5-EF) at the N-terminus of the 85 kDa polypeptide chain and then a short polybasic region (PRBN) that localizes the enzyme to the PtdIns(4,5)P_2-rich plasma membrane (*5*), followed by the domains common to all NOXes, i.e., the six helix-containing transmembrane region, and finally the catalytic dehydrogenase domain (CDHD) which contains the sites for FAD (two subregions) and for NADPH (four subregions) (Figure 1).

NOX5 genes occur in the genomes of metazoans such as the sea anemone, the limpet, insects, and most vertebrates, except for rodents. The single human NOX5 gene is expressed as five alternatively spliced forms: α, β, the minor δ and γ forms, and a short form (NOX5-S) that lacks the entire EF-hand region (*6*). NOX5α is strongly expressed in the spleen, NOX5β in the testis, and NOX5-S in most fetal tissues, adenocarcinoma cells, and microvascular endothelial cells (*6*).

In humans several biological and pathological functions of NOX5 have recently been described (*6*). The protooncogene cAbl appears to be a NOX5-binding protein, suggesting a role in cell growth and signaling (*7*). NOX5-derived superoxide enhances cell growth of prostate cancer (*8*) and of malignant B cells (*9*) and PDGF-induced proliferation in human aortic smooth muscle (*10*). NOX5 protein and mRNA levels are highly upregulated in coronary artery disease (*11*). NOX5 is active in vascular endothelial cells, where the Ca^{2+} levels are always relatively elevated and low levels of superoxide are always produced. It seems that the highly localized production of superoxide and its subsequent local action on target proteins are the bases for the specific action of each of the NOX isoforms in protein transcription and cell signaling.

NOX5 does not require other membranous or cytosolic activator proteins but is activated by an increase in the concentration of cytoplasmic Ca^{2+} (*12*). The relative high $[Ca^{2+}]_{0.5}$ corresponding to the half-maximal superoxide production of 1 μM can be explained by the fact that NOX5 is a plasma membrane protein (*5*): it is well-known that the increase in Ca^{2+} concentration within submembranous microdomains may exceed that of the cytoplasm by orders of magnitude (*13*). Moreover, the Ca^{2+} sensitivity of NOX5 can be fine-tuned by two recently discovered sophistications: (1) PKC phosphorylation increases the sensitivity of NOX5 to intracellular $[Ca^{2+}]$ and enhances the duration of the Ca^{2+}-dependent production by

[†]This work was supported by a grant from the Swiss National Science Foundation, 3100AQ-108215/1.

*Address correspondence to these authors. Fax: 0041 22 3796470. Tel: 0041 22 3796491. E-mail: jos.cox@unige.ch; fabiana.tirone@unige.ch.

[1]Abbreviations: NOX, NADPH oxidase; CDHD, catalytic dehydrogenase domain of NOX5; FAD, flavin adenine dinucleotide; GST, glutathione *S*-transferase; NADPH, nicotinamide adenine dinucleotide phosphate; NOX5-EF, amino acid 1−169 region of NOX5; CaM, calmodulin; REFBD, regulatory EF-hand-binding domain; PhosR, phosphorylatable region; PBS, phosphate-buffered saline; BAPTA, 1,2-bis(2-aminophenoxy)ethane-*N*,*N*,*N*′,*N*′-tetraacetic acid; NTA, nitrilotriacetic acid; SOD, superoxide dismutase; PAGE, polyacrylamide gel electrophoresis; SDS, sodium dodecyl sulfate; DSS, disuccinimidyl suberate.

Published on Web 12/22/2009

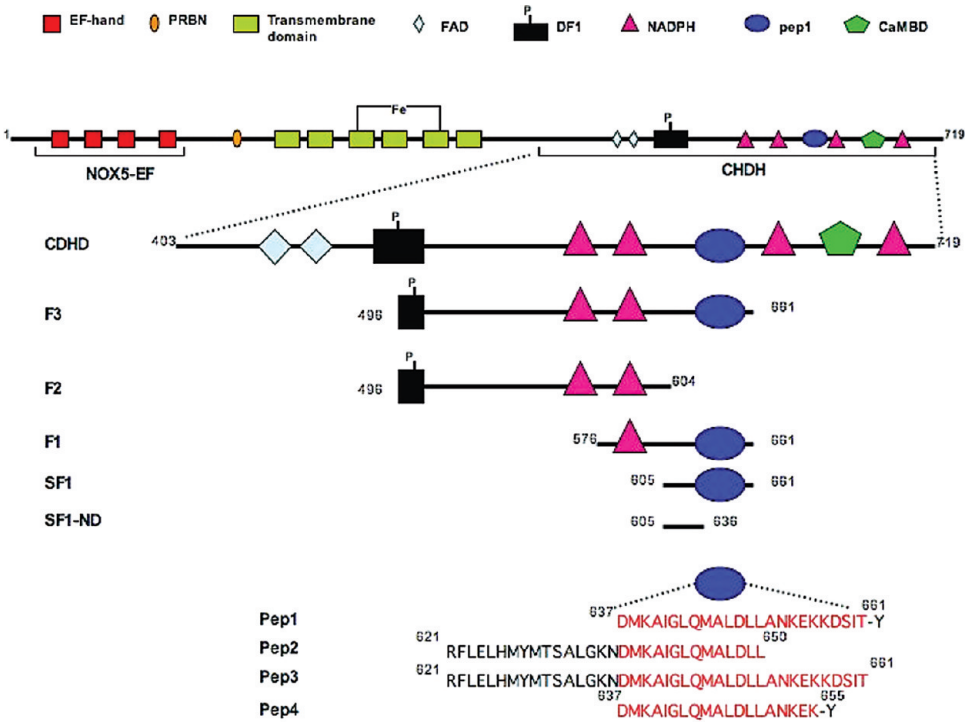

FIGURE 1: Diagram of the domain structure of human NOX5. The linear structure of the cytoplasmic dehydrogenase domain (CDHD) is blown up and below it are presented the designed protein constructs (F3 to SF1-ND) and peptides (pep1 to pep4) used in this work. Abbreviations: PRBN, polybasic region; CaMBD, calmodulin-binding domain; DF1, phosphorylatable region.

NOX5 (*14*). (2) We showed that CaM also increases the sensitivity of the enzyme for Ca^{2+}. CaM decreases the K_m by a factor of 10 (*15*).

In molecular terms the activation mechanism implies that the NOX5-EF domain binds four Ca^{2+}, undergoes conformational changes including the exposure of a hydrophobic surface, and interacts with the catalytic C-terminal domain, which leads to its activation, i.e., either induction of the catalytic site or release of an inhibitory segment. The former model is operational in the calpains (*16*); the latter is the consensus mechanism for activation of canonical targets by calmodulin (CaM) (*17*). The aim of this study is to investigate how NOX5-EF interacts with the catalytic CDHD (Figure 1): if it interacts with a single short segment as in the case of the majority of calmodulin targets (*18*, *19*) or if there are more segments that interact with a single NOX5-EF domain as occurs in some calmodulin (*20*) and S100A6 targets (*21*). We also discussed the relationship of this basal activation mechanism to the two above-described enhancing mechanisms.

MATERIALS AND METHODS

Materials. Anti-NOX5-EF antibodies were kindly provided by Dr. Botond Bánfi.

Peptides pep1 (D637−G661 + Y), pep1′ (acetylated and amidated pep1), pep2 (R621−L650), pep3 (R621−T660), and pep4 (D637−E654 + Y) were purchased from CMU (Centre Medical Universitaire, Geneva, Switzerland). The purity was above 95% as assessed by high-pressure liquid chromatography analysis. Peptide DF1 (L489−S505) was kindly provided by the Fulton group from the Medical School of Georgia, Augusta.

Plasmid Constructs. All DNA constructs encoding the CDHD (M403−F719), F3 (R496−G661), F2 (R496−V604), F1 (I576−T660), SF1 (S605−T660), and SF1-ND (S605−N636) of the C-terminus of NOX5 were generated from human NOX5β cDNA by PCR, cloned into pGEX-2T vector, and verified by sequencing (Fasteris, Geneva, Switzerland). The following primers (forward and reverse, respectively) were used in the PCR experiments: 5′-ctggatcccgaaagagtcaaaggtcgtcc-3′ and 5′-ctgaattccgtgatggagtctttcttc-3′ for F3, 5′-ctggatcccgaaagagtcaaaggtcgtcc-3′ and 5′-ctgaattcacaaaccactcgaaagacc-3′ for F2, 5′-ctggatcccagatcgaaggtgtccaagaca-3′ and 5′-ctgaattccgtgatggagtctttcttc-3′ for F1, 5′-ctggatccagcctgctgactaaactgg-3′ and 5′-ctgaattccgtgatggagtctttcttc-3′ for SF1, and 5′-ctggatccagcctgctgactaaactgg-3′ and 5′-ctgaattcgtcattcttgcccagtgc-3′ for SF1-ND.

Protein Expression and Purification. All DNA constructs encoding recombinant CDHD, F3, F2, F1, SF1, and SF1-ND were transformed in *Escherichia coli* BL21 p-Lys bacteria. Protein expression was induced by 4 h incubation with 500 μM IPTG at 37 °C. The glutathione *S*-transferase (GST) fusion proteins were purified as previously described (*15*, *22*). The purity of all recombinant fusion proteins was verified by SDS−PAGE in 15% gels. All pull-down experiments have been done using the glutathione−agarose-bound fusion protein. It must be underlined that since these proteins constructs were completely insoluble in the absence of GST, no other methods of complex monitoring could be applied. After or during purification all of the recombinant proteins underwent spontaneous proteolysis even in the presence of a cocktail of protease inhibitors.

Pull-Down Experiments. The Ca^{2+}-dependent interaction of NOX5-EF with different constructs of the C-terminus of NOX5 was analyzed by the pull-down technique followed by direct Coomassie staining or Western blotting as described before (*15*, *22*). Briefly, 100 μg of GST-CDHD, GST-F3, GST-F2, GST-F1, GST-SF1, and GST-SF1-ND on glutathione−agarose beads was incubated with 100 μg of NOX5-EF in the presence of 1 mM $CaCl_2$ or EGTA for 1 h at room temperature. After centrifugation the supernatant was removed, and the beads were washed with ten times their volume of 50 mM Tris-HCl, pH 7.5, and 150 mM NaCl containing respectively

1 mM $CaCl_2$ or 1 mM EGTA in the presence of protease inhibitors. At the end, sample buffer was added, and the samples were boiled for 10 min and analyzed by SDS−PAGE in 15% gels. After transfer of the proteins (1 h, 120 V at 4 °C), the membrane was blocked overnight with 1× PBS, 0.5% milk, and 0.5% Tween 20. Then the membrane was incubated for 1 h at room temperature with anti-NOX5-EF antibodies, washed, and incubated with the anti-rabbit HRP-labeled antibodies (Promega). The proteins were detected using ECL solution (Amersham). A previously shown control experiment showed that the GST−agarose beads alone do not interact with NOX5-EF (*22*).

Covalent Cross-Linking. Cross-linking experiments between NOX5-EF and different ratios of five synthetic peptides from the C-terminal domain of NOX5 (namely, pep1, pep2, pep3, pep4, and DF1) were performed at room temperature as described earlier (*23*). Briefly, 6 μg of NOX5-EF in 25 mM $(NH_4)HCO_3$, pH 7.5, in the presence of 1 mM $CaCl_2$ or 1 mM EGTA was incubated at different ratios with the synthetic peptides in the presence of 100 μM disuccinimidyl suberate (DSS); after 3 h at room temperature, the reaction was stopped by adding 1 mM ethanolamine. The samples were analyzed by SDS−PAGE in 17.5% gels.

Isothermal Titration Calorimetry. Thermodynamic parameters of molecular interactions between NOX5-EF and target peptides were investigated by ITC using a MicroCal VP-ITC instrument (MicroCal Inc., Northampton, MA). The proteins and peptides were equilibrated in buffer containing 50 mM Mops (pH 7.4), 100 mM NaCl, and 2 mM $CaCl_2$ or 2 mM EDTA. The NOX5-EF at 15−30 μM in the calorimeter cell was titrated by the peptide (ca. 250 μM stock solution) by automatic injections of 8−10 μL. The first injection of 2 μL was ignored in the final data analysis. Integration of the peaks corresponding to each injection and correction for the baseline were done using Origin-based software provided by the manufacturer. The fit of the data to a single-site interaction model results in the stoichiometry (n), association constant (K_a), and enthalpy of complex formation (ΔH). All of the experiments were repeated twice and give similar results. Control experiments, consisting in injecting peptide solutions into the buffer, were performed in order to evaluate the heat of dilution. For reason of limited solubility of pep2, this interaction could not be monitored.

Fluorescence Spectroscopy. Trp fluorescence spectra and isotherms were measured at 20 °C using a Perkin-Elmer LS 50B spectrofluorometer as described earlier (*24*). For interactions with NOX5-EF the excitation wavelength was at 280 nm, and emission spectra were recorded from 310 to 380 nm. Slits were at 5 nm. The dissociation constants were calculated iteratively (MatLaB) with the use of eq 2 in ref *25*.

Membrane Preparation. Membranes of NOX5 and control-transfected HEK293 cells were prepared as described before (*22*). Briefly, cells were resuspended in 10% sucrose, 0.2× PBS, pH 7.5, 120 mM NaCl, 5 mM EGTA, and 1 tablet of protease inhibitors complete EDTA-free from Roche and broken by sonication. After sonication they were centrifuged at 200*g* for 10 min, and the supernatant was layered onto a 17%/40% (w/v) discontinuous gradient and centrifuged at 150000*g* for 30 min. The membrane fractions were collected from the 17%/40% interface. Protein concentrations were determined by Bradford reagent using BSA as a standard.

NADPH Oxidase Activity Assays. In the cell-free system superoxide generation was measured with a chemiluminescence assay MCLA (with 2-methyl-6-(4-methoxyphenyl)-3,7-dihydroimidazo[1,2-*a*]pyrazin-3(7*H*)-one hydrochloride) using FluoSTAR OPTIMA (BMG Labtech). Four micrograms of membrane protein was prepared in a final volume of 150 μL/well in the presence of 50 mM HEPES, pH 7.5, 0.3 mM NTA, 0.3 mM HEDTA, 0.3 mM BAPTA, 10 μM FAD, 1 mM $MgCl_2$, 5.5 μM phosphatidic acid (1,2-didecanoyl-*sn*-glycerol 3-phosphate; Sigma), 50 μg/mL MCLA, and 700 μM $CaCl_2$, and various concentrations of pep3, pep5, and DF1 were added. We used a mixture of three different Ca^{2+} buffers (BAPTA, HEDTA, and NTA) to accurately control the free $[Ca^{2+}]$ in the system. All experiments were carried out at free $[Ca^{2+}]$ of 50 μM. The reaction were performed at 37 °C and initiated by adding 200 μM NADPH (the K_m for NADPH is 30 μM; F. Tirone, data not shown). Superoxide generation was determined by measuring the MCLA emission at 590 nm. Routinely, control assays were done in the presence of SOD (*21*).

Controlled Proteolysis of NOX5-Transfected Membranes. The tryptic digestion of NOX5 (1/500 enzyme/protein) was carried at 37 °C in 10% sucrose, 0.2× PBS, pH 7.5, 120 mM NaCl, and 5 mM EGTA, pH 8, during 45 min. The reaction was stopped by adding protease inhibitors complete EDTA-free from Roche. Aliquots were picked up at different times, and their enzymatic activity was tested in the cell-free system.

RESULTS

Ca^{2+}-Dependent Binding of NOX5-EF to Three Different Fragments of the NOX5 C-Terminus. In search for the regulatory EF-hand-binding domain (REFBD) in the catalytic domain of NOX5 we used different GST constructs to perform pull-down experiments (Table 1). The GST-CDHD (residues M403−F719), GST-F3 (R496−G661), GST-F2 (R496−V604), and GST-F1 (I576−G661) immobilized on glutathione−agarose beads were incubated with NOX5-EF in the presence or absence of 1 mM $CaCl_2$; 100 μg of each recombinant fusion protein was mixed with 100 μg of NOX5-EF at room temperature and then washed, and samples were analyzed by SDS−PAGE followed by Coomassie staining. NOX5-EF was able to bind to the full GST-CDHD (confirming the data in ref *22*), to GST-F3, and to GST-F1 fusion proteins. No interaction was detected with the GST-F2 fusion protein (data not shown). All interactions required the presence of Ca^{2+} (Figure 2).

Next we cloned and expressed the recombinant construct GST-SF1 (residues S605−G661), corresponding to a shorter form of the GST-F1 which lacks the overlapping region between F1 and F2. We performed again pull-down assays including GST-SF1 immobilized on glutathione−agarose beads and incubated with NOX5-EF in the presence or absence of 1 mM $CaCl_2$ (Figure 2B); the samples were analyzed by SDS−PAGE followed by Western blotting with anti-NOX5-EF antibody as described in Materials and Methods. As shown in Figure 2B NOX5-EF binds also to SF1, and the different interacting fragments show bands of almost the same intensities, demonstrating that the REFBD resides in the segment S605−T660 of the CDHD.

Ca^{2+}-Dependent Complex Formation between NOX5-EF and Peptides pep1, pep2, pep3, and pep4. To narrow down the REFBD, we decided to synthesize peptides of different lengths in the region S605−T660 of the CDHD of NOX5 and to test also the peptide DF1, kindly provided by Fulton's group, corresponding to the phosphorylation region (*13*).

The choice of the peptides was based on the comparison of the sequences of NOX2 and NOX5 in the region of the fragment SF1 (S605−T660). Indeed, Taylor et al. (*26*) have modeled the

Table 1[a]

A. Sequence of CDHD of NOX5 and five cloned fragments probed by pull down.

CDHD:
^{403}MEVNLLPSKVTHLLIKRPPFFHYRPGDYLYLNIPTIARYEWHPFTISSAPEQKDTIWLHIRSQG
QWTNRLYESFKASDPLGRG**SKRLSRSVTMRKSQRSSKGS**EILLEKHKFCNIKCYIDGPYGTPTRRI
FASEHAVLIGAGIGITPFASILQSIMYRHQKRKHTCPSCQHSWIEGVQDNMKLHKVDFIWINRDQR
SFEWFVSLLTKLEMDQAEEAQGRFLELHMYMTSALGKN***DMKAIGLQMALDLLANKEKKDSIT***GLQT
RTQPGRPDWSKVFQKVAAEKKGKVQVFFCGSPALAKVLKGHCEKFGFRFFQENF^{719}

F3:
^{496}RKSQRSSKGSEILLEKHKFCNIKCYIDGPYGTPTRRIFASEHAVLIGAGIGITPFASILQSIMY
RHQKRKHTCPSCQHSWIEGVQDNMKLHKVDFIWINRDQRSFEWFVSLLTKLEMDQAEEAQGRFLEL
HMYMTSALGKNDMKAIGLQMALDLLANKEKKDSITG^{661}

F2:
^{496}RKSQRSSKGSEILLEKHKFCNIKCYIDGPYGTPTRRIFASEHAVLIGAGIGITPFASILQSIMY
RHQKRKHTCPSCQHSWIEGVQDNMKLHKVDFIWINRDQRSFEWFV^{604}

F1:
^{576}IEGVQDNMKLHKVDFIWINRDQRSFEWFVSLLTKLEMDQAEEAQGRFLELHMYMTSALGKNDMK
AIGLQMALDLLANKEKKDSITG^{661}

SF1:
^{605}SLLTKLEMDQAEEAQGRFLELHMYMTSALGKNDMKAIGLQMALDLLANKEKKDSITG^{661}

SF1-ND:
^{605}SLLTKLEMDQAEEAQGRFLELHMYMTSALGKN^{636}

B. Sequence of five synthetic peptides probed by cross-linking, fluorescence and ITC.

pep4: ^{637}DMKAIGLQMALDLLANKEK^{655}Y

pep3: ^{621}RFLELHMYMTSALGKNDMKAIGLQMALDLLANKEKKDSIT^{660}

pep2: ^{621}RFLELHMYMTSALGKNDMKAIGLQMALDLL^{650}

pep1: ^{637}DMKAIGLQMALDLLANKEKKDSITG^{661}Y

DF1: ^{489}LSRSVTMRKSQRSSKGS^{505}

The Y (red) in pep1 and 4 was added to facilitate the determination of the peptide concentration. In blue: FAD-binding subregions; in red: NADPH-binding subregions; bold: phosphorylatable region (PhosR); bold italic: regulatory EF-binding domain (REFBD); underlined: CaM-binding domain (CaMBD)

[a]The Y (red) in pep1 and pep4 was added to facilitate the determination of the peptide concentration. In blue, FAD-binding subregions; in red, NADPH-binding subregions; bold, phosphorylatable region (PhosR); bold italic, regulatory EF-binding domain (REFBD); underlined, CaM-binding domain (CaMBD).

tridimensional structure of the catalytic dehydrogenase of NOX2 on the basis of ferrodoxin−NADP reductase which bears important sequence similarity to the CDHD (*27*) and which has been crystallized with the two bound nucleotides FAD and NADPH (*28*). Taylor et al. pointed out that NOX2 CDHD contains an α-helical insert which is not present in the nonregulated ferrodoxin. Several considerations led Taylor to the hypothesis that this α-helix is the regulated element in NOX2. The sequence alignment of this putative regulated segment in different NOXes revealed that NOX1, NOX2, and NOX3 show high similarity, but not NOX5 (Table 2A). In the latter enzyme this segment extends from D637 to T660 just before the third segment LQTRT implicated in NADPH binding (Table 1, bold italic); it is predicted to be α-helical from D637 to E654. These structural deductions brought us to synthesize pep1 (D637−G661 plus a C-terminal Tyr residue), pep2 (R621−L650), pep3 (R621−T660), and pep4 (D637−E656 plus a C-terminal Tyr residue) as seen in Table 1B. Covalent cross-linking experiments were performed with NOX5-EF and different ratios of pep1, pep2, pep3 and DF1 in the presence or absence of 1 mM $CaCl_2$. In the presence of the covalent cross-linker DSS, the Ca^{2+} form of NOX5-EF forms a dimer, but not the metal-free form. In the presence of $CaCl_2$ strong complex formation was observed for pep1 and pep3 and very weak complex formation for pep2 (Figure 3A); pep3 reacted weakly also in the absence of Ca^{2+} (Figure 3B). For the others no interaction was detected in the presence of EGTA (Figure 3B). For pep4 no interaction was detected either in $CaCl_2$ or in EGTA (data not shown). It should be underlined that pep4 and pep1 differ by only five amino acid residues, i.e., KKDSIT, from which one can deduce that this short stretch must be much more important for the binding of NOX5-EF than the longer N-terminal-ward stretch. DF1 reacted very weakly only in presence of Ca^{2+} (Figure 4). The molecular weight of the complexes indicated a 1:1 stoichiometry.

Complex Formation Monitored by Trp Fluorescence. In order to evaluate the conformational changes in NOX5-EF upon interaction with the synthetic peptides, we monitored the fluorescence of the conformation-sensitive Trp residues. NOX5-EF possesses three Trp (W9 and W12 in the N-terminal half and W165 in the C-terminal half). When increasing concentrations of

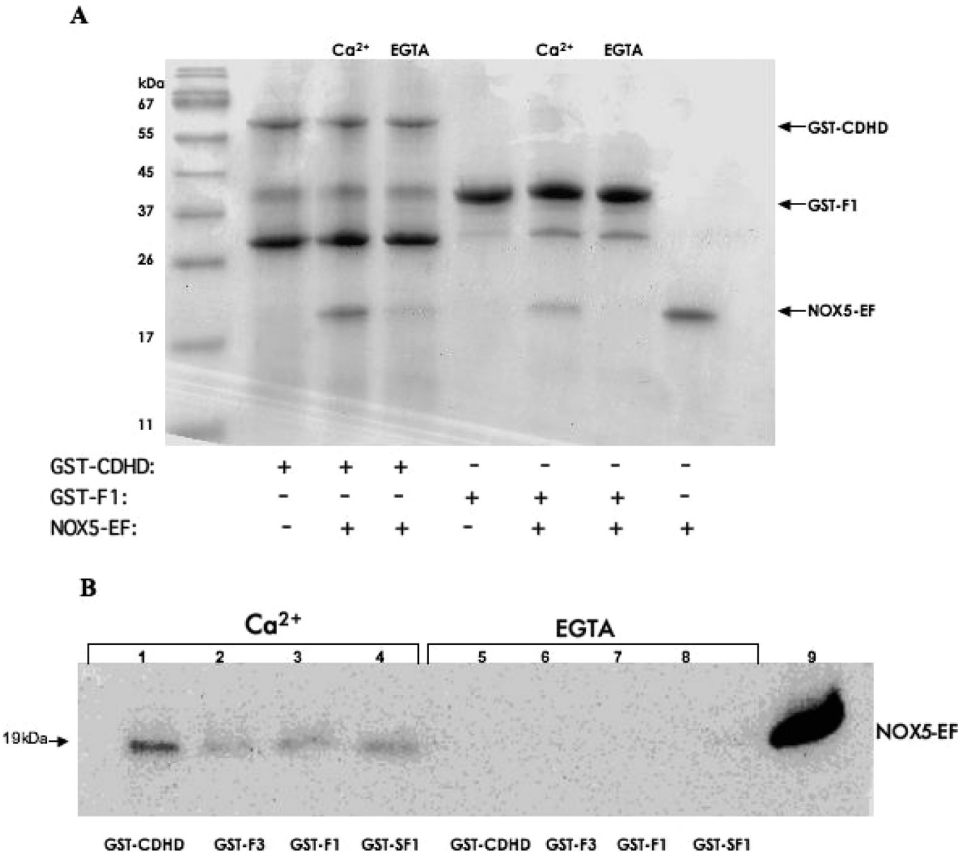

FIGURE 2: Ca^{2+}-dependent interaction of NOX5-EF with the GST-CDHD and GST-F1 checked by pull down and 15% SDS−PAGE. (A) The GST-CDHD and GST-F1 fusion proteins of the NOX5 C-terminus on glutathione−agarose beads were mixed with NOX5-EF in the presence of 1 mM $CaCl_2$ or 1 mM EGTA and washed in the presence or absence of Ca^{2+}. The samples were revealed by Coomassie staining. NOX5-EF binds to both recombinant proteins in a Ca^{2+}-dependent manner (lanes 3 and 6); no interaction is detected in the absence of Ca^{2+} (lanes 4 and 7). Lanes 2, 4, and 8 represent controls of GST-CDHD, GST-F1, and NOX5-EF, respectively. The 30 kDa band and the less intense one at ca. 40 kDa result from the endogenous proteolysis of the proteins. (B) Ca^{2+}-dependent interaction of NOX5-EF with GST-CDHD, GST-F3, GST-F1, and GST-SF1 checked by pull down followed by Western blotting. NOX5-EF binds to the four recombinant proteins in a Ca^{2+}-dependent manner (lanes 1, 2, 3, and 4); in the absence of Ca^{2+} no signal was detected (lanes 5, 6, 7, and 8); lane 9, control NOX5-EF.

Table 2[a]

A. Putative regulated segment in NOXes.

```
hNOX1   FLNYRLFLTGWDS----NIVGHAALNFDKATDIVTGLKQKTSF
hNOX2   FLSYNIYLTGWDE----SQANHFAVHHDEEKDVITGLKQKTLY
hNOX3   FLSYHIFLTGWDE-----QALHIALHWDENTDVITGLKQKTFY
hNOX4   YVNIQLYLSQTDG----IQKIIGEKYH--------ALNSRLFI
hNOX5   HMYMTSALGKNDMKAIGLQMALDLLANKEKKDSITGLQTRTQP
```

B. REFBD of NOX5 of different species

```
                    1  4    8    12
HUMAN               DMKAIGLQMALDLLANKEKKDSIT
BOVIN               DIKAIGLQMALDLLAKKEKKDSIT
OPOSSUM             DMKAIGLQMALDLLAKKENKDSIT
DOG                 DMKAIGLQMALDLLAKKEKKDSIT
CHICK               DVKAVGLQLALDLLAAKEQRDSIT
ZEBRA FISH          DMKAIGLQMALDLLAKKEKRDSIT

LOTTIA G.           DMKGIGLQVALDLIHEKEQRDLLT
CAPITELLA SP.       DMKGIGLQVALDLIHEKEQRDLLT
HONEY BEE           DMKAVTLQLAMDLVHQMEKRDLIT
```

In red: the third NADPH-binding subregion; in bold: the predicted regulated element in NOX5 (REFBD). Boxed is the putative regulated segment proposed by Taylor et al. for NOX2. Not conserved amino acids are underlined.

[a]In red, the third NADPH-binding subregion; in bold, the predicted regulated element in NOX5 (REFBD). Boxed is the putative regulated segment proposed by Taylor et al. for NOX2. Not conserved amino acids are underlined.

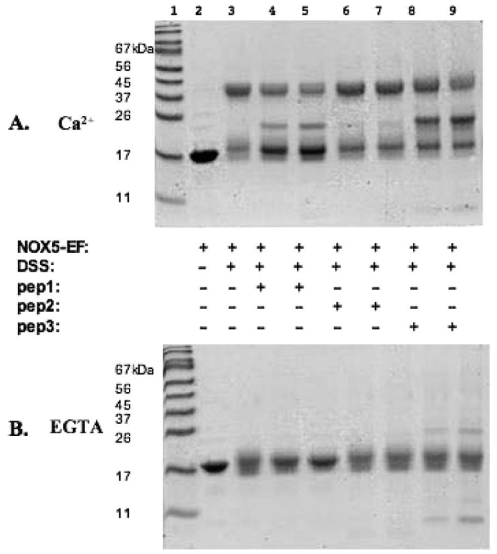

FIGURE 3: Ca^{2+}-dependent complex formation between NOX5-EF and pep1, pep2, and pep3 analyzed by covalent cross-linking with DSS, followed by 17.5% SDS−PAGE. NOX5-EF was incubated with two different ratios of pep1, pep2, and pep3 in the presence of 1 mM Ca^{2+} (panel A) and 1 mM EGTA (panel B). Key: lane 2, NOX5-EF; lane 3, NOX5-EF + DSS; lane 4, NOX5-EF + pep1 (1:1) + DSS; lane 5, NOX5-EF + pep1 (1:2) + DSS; lane 6, NOX5-EF + pep2 (1:1) + DSS; lane 7, NOX5-EF + pep2 (1:2) + DSS; lane 8, NOX5-EF + pep3 (1:1) + DSS; lane 9, NOX5-EF + pep3 (1:2) + DSS;. C, complex; D, dimer.

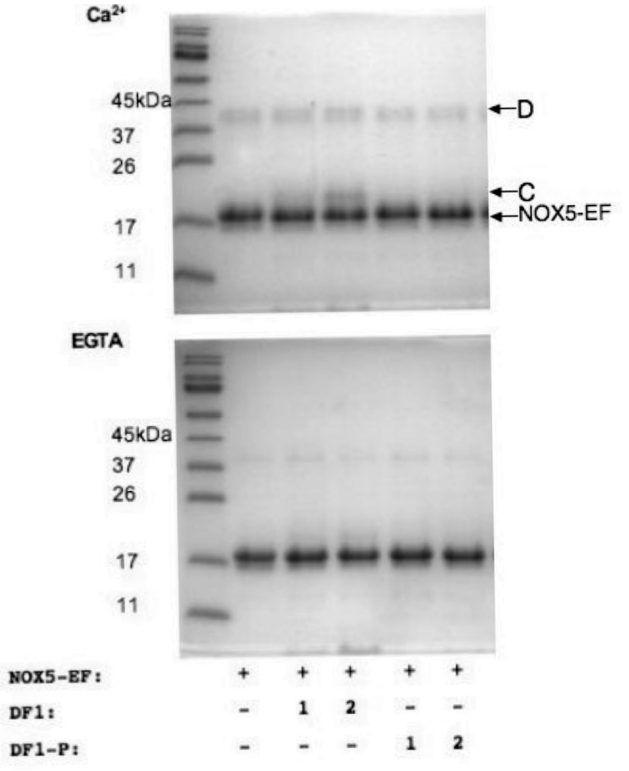

FIGURE 4: Monitoring of Ca^{2+}-dependent complex formation between NOX5-EF and peptide DF1 by covalent cross-linking with DSS and 17.5% SDS−PAGE. The peptides were either phosphorylated (DF1-P) or nonphosphorylated (DF1). All lanes contain 6 μg of NOX5-EF, 1 mM $CaCl_2$ or EGTA, and 100 μM DSS. Gel Ca^{2+}: lane 1, standards; lane 2, NOX5-EF + DSS; lane 3, NOX5-EF + DF1 (1:1); lane 4, NOX5-EF + DF1 (1:2); lane 5, NOX5-EF + DF1-P (1:1); lane 6, NOX5-EF + DF1-P (1:2); C, complex; D, dimer. Same for the gel in EGTA.

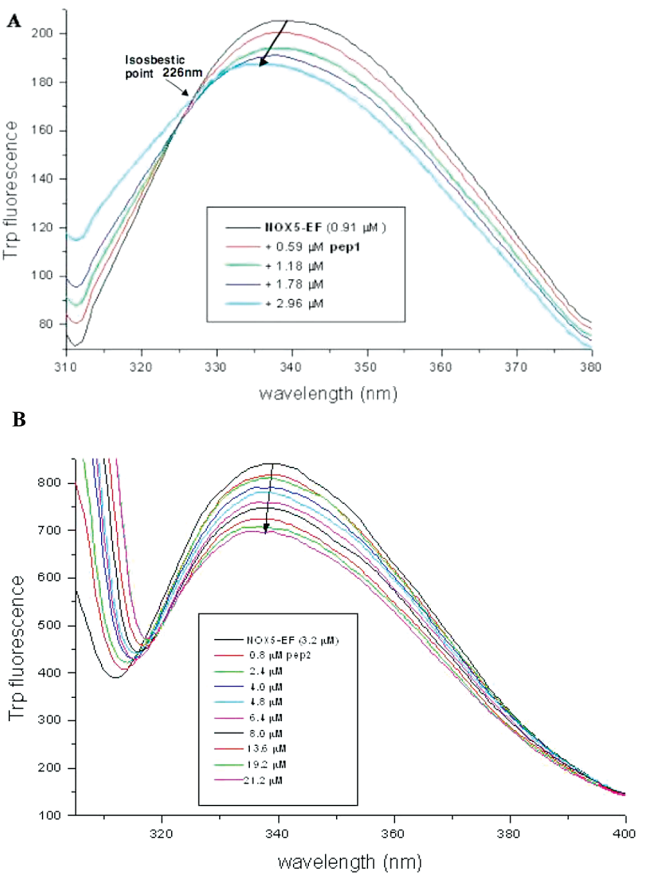

FIGURE 5: Interaction of NOX5-EF with pep1 (A) and pep2 (B) measured by Trp fluorescence. The concentrations of NOX5-EF and added peptide are indicated in the inserts.

pep1 were added to 0.9 μM NOX5-EF in buffer A (50 mM Tris-HCl, pH 7.5, 150 mM KCl) containing 1 mM Ca^{2+}, the Trp fluorescence intensity decreased by 21% at 345 nm. Moreover, a blue shift of 5 nm of the maxima occurred together with an isosbestic point at 226 nm (cross-point in Figure 5A). From this fluorescence change we estimated, as described in Materials and Methods, a dissociation constant (K_d) of ca. 1 μM for the complex NOX5-EF/pep1. No fluorescence change was observed in the presence of 1 mM EGTA instead of Ca^{2+} (data not shown). The interaction of pep2, which is located N-terminally of pep1 with an overlap of 14 residues, with NOX5-EF was accompanied by a fluorescence decrease at 338 nm of 15%, but a very weak wavelength shift and no clear isosbestic point were observed (Figure 5B). A K_d of 5 μM was estimated. The pep1 blocked at its C- (-acetyl) and N- (amide-) termini (i.e., pep1′) showed the same properties as the nonblocked pep1. For pep3 and pep4 no Trp fluorescence change was observed in similar titration experiments.

Microcalorimetry. Using the ITC technique NOX5-EF was titrated with the different peptides in the presence and absence of Ca^{2+}, and the data are summarized in Table 3. Pep1 interacts in a 1:1 stoichiometry (Figure 6A) with NOX5-EF, and fitting of the integrated data to a one-site binding model results in a K_d of 2−3 μM with a rather low negative enthalpy change (ca. −2 kcal/mol). Thus the entropy term is the more important driving force, and the gain in structure upon complex formation is rather low. This was confirmed by circular dichroism experiments: the far-UV spectrum of NOX5-EF was not notably changed by the addition of pep1 (C. T. Craescu, data not shown). Table 3 shows that an

N-terminal extension of the peptide (pep3) does not improve the affinity significantly. The higher binding enthalpy of this longer peptide is probably compensated by a larger contribution of the unfavorable conformational entropy contribution. However, the C-terminal truncation (pep4) leads to a 2−3-fold decrease of the affinity, thus validating the status of pep1 as the representative target model of NOX5-EF in its interaction with the catalytic domain. In the absence of Ca^{2+} no interaction could be measured (Figure 6B). This high Ca^{2+} dependence indicates that NOX5 does not expose its hydrophobic surface in the absence of the divalent cation. As expected, the enthalpy/entropy values of the other synthetic peptides are quite similar (Table 3). The somewhat lower affinity of pep4 is due to a lower gain of entropy.

Ca^{2+}-Dependent Interaction of NOX5-EF with GST-SF1-ND Compared to GST-CDHD, GST-F1, and GST-SF1. To confirm that pep1 was the real main part of the REFBD of NOX5, we cloned a new recombinant protein, SF1-ND (S605−N636; see Table 1). This construct is a shortened form of the SF1 protein, lacking 23 residues at the C-terminal sequence corresponding to pep1. We performed pull-down assays with GST-CDHD, GST-F1, GST-SF1, and GST-SF1-ND immobilized on glutathione−agarose beads and incubated with NOX5-EF in the presence or absence of 1 mM $CaCl_2$. Samples were analyzed by SDS−PAGE followed by Coomassie staining. As shown in Figure 7A, NOX5-EF did not bind to the GST-SF1-ND recombinant protein, in contrast to the other fragments of the C-terminus.

To see if the interaction was abolished, we performed pull-down experiments between the GST-CDHD and NOX5-EF in the presence of pep1. As shown in Figure 7B the Ca^{2+}-dependent interaction of NOX5-EF with GST-CDHD is strongly reduced by the presence of pep1, confirming that the segment D637−T660 corresponds to the REFBD in the catalytic C-terminal domain of NOX5. We tested pep3 and DF1, and the competitive interaction was less pronounced likely due to their lower affinity for NOX5-EF; pep4 had no effect on the interaction between NOX5-EF and the GST-CDHD.

Investigation of the Effect of pep1, pep3, and DF1 on the Superoxide Production by NOX5. After identification of the two regions in the CDHD that interact with the regulatory domain of NOX5, we decided to evaluate the role of these segments on the enzymatic activity. Therefore, we performed the cell-free system assay using NOX5-containing membranes in the presence of the different peptides. Previously, we reported that NOX5 activation was strongly dependent on free Ca^{2+} concentration in the 0.3−7 μM range (*22*), and this was confirmed here. In the present study, we added to the system the peptides DF1, pep1, and pep3 at different concentrations (Figure 8); NOX5 superoxide generation was inhibited up to 90% (of maximal activation) by pep1 and pep3 at the concentration of 300 μM, with no major differences, and the half-maximal inhibition is at

Table 3

protein	ligand	2 mM Ca^{2+}	K_a (error) ($\times 10^5$ M^{-1})	ΔH (error) (kcal/mol)	$T\Delta S$ (kcal/mol)
NOX5-EF	pep1	with	4.7 (0.5)	−1.9 (0.7)	6.0
NOX5-EF	pep1	without	NB[a]		
NOX5-EF	pep3	with	4.0 (0.6)	−6 (0.05)	1.8
NOX5-EF	pep3	without	NB[a]		
NOX5-EF	pep4	with	1.4 (0.2)	−3.6 (0.03)	3.5
NOX5-EF	pep4	without	NB[a]		
NOX5-EF	pep1′	with	3.2 (0.7)	−3.1 (0.3)	4.5
NOX5-EF	pep1′	without	NB[a]		

[a]No binding; K_a = equilibrium association constant.

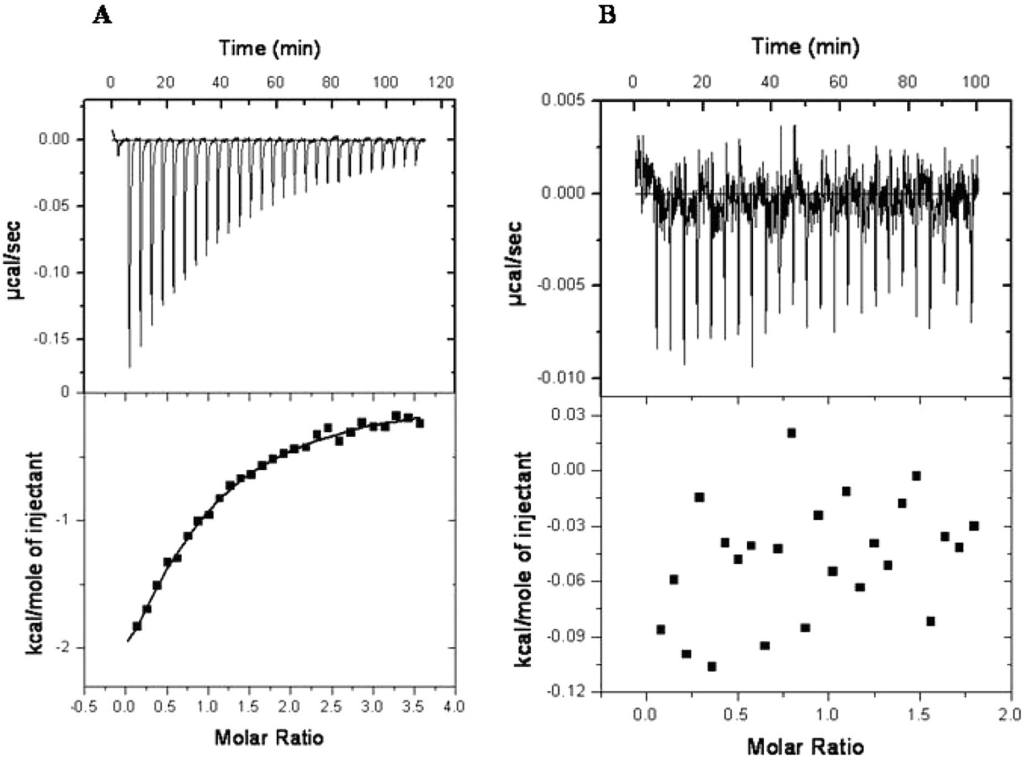

FIGURE 6: Calorimetric data for pep1 binding to NOX5-EF. Experimental traces of the titration of 30 μL of NOX5-EF with pep1 in the presence of 2 mM Ca^{2+} (A) or EDTA (B) are shown in the top panel, and the integrated binding isotherms are shown in the bottom panel. In (A) K_d = $(4.8 \pm 0.5) \times 10^5$ M^{-1}, $n = 0.77 \pm 0.06$, and $\Delta H = 1.9 \pm 0.7$ kcal/mol. In (B) no interaction was observed.

30 μM. To reach the same inhibition with DF1, its concentration had to be increased to 1 mM, and the half-maximal inhibition is at 160 μM. Then we measured the dose−response of superoxide production by NOX5 to pep1 in the presence of DF1, but no increase in sensitivity was observed (data not shown). All of these data confirm that the regulatory N-terminal domain of NOX5-EF binds to the CDHD of NOX5 in these now well-defined regions and that the activation of the enzyme is dependent on this interaction.

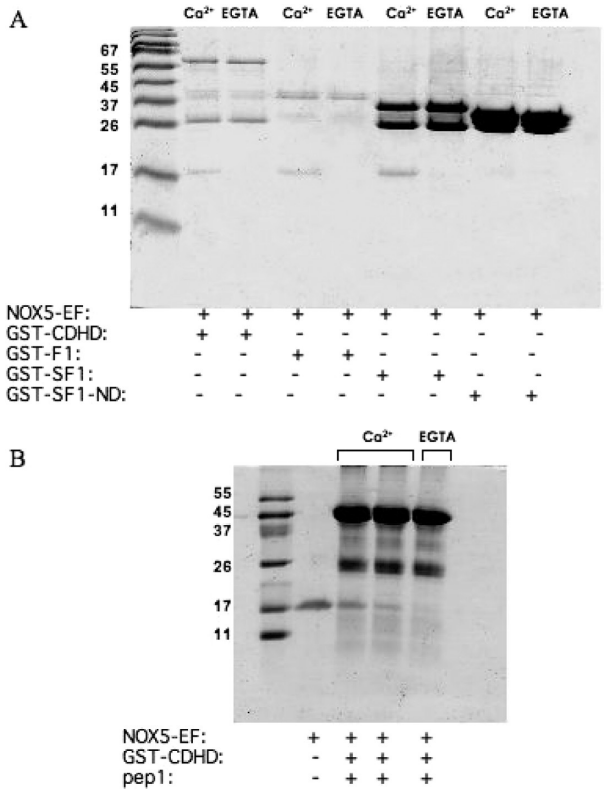

FIGURE 7: (A) Ca^{2+}-dependent interaction of NOX5-EF with GST-CDHD, GST-F1, GST-SF1, and GST-SF1-ND checked by pull down followed by 15% SDS−PAGE. The GST-CDHD, GST-SF1, and GST-SF1-ND on glutathione−agarose beads were incubated with NOX5-EF in the presence or absence of 1 mM Ca^{2+}. NOX5-EF binds in a Ca^{2+}-dependent way only to the GST-CDHD, GST-F1, and GST-SF1 recombinant proteins (lanes 2, 4, and 6); no interaction occurs with GST-SF1-ND protein in the presence (lane 8) or absence (lane 9) of Ca^{2+}. (B) The Ca^{2+}-dependent interaction of NOX5-EF with the GST-CDHD (lane 3) was partially reversed by pep1 (lane 4).

Elucidation of the Activation Mechanism of NOX5. The activation of several enzymes by CaM implies the removal of an autoinhibitory element that blocks the catalytic site. An alternative way to activate these enzymes is to remove the autoinhibitory element by controlled proteolysis or with the help of organic solvents, as in the case of the calcium-pumping ATPase (*29*), cyclic nucleotide phosphodiesterase (*30*), and phosphorylase kinase (*31*, *32*). To elucidate the mechanism of activation of NOX5 and see if the REFBD has an autoinhibitory role, we performed a controlled trypsinolysis on NOX5-containing membranes. During a time course of 45 min, membrane samples were taken away at different times, and the enzymatic activity was measured in the absence of Ca^{2+}. As shown in Figure 9, without proteolysis or at a very short time (< 3 min) of

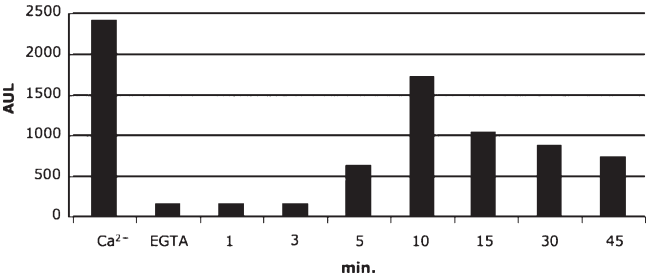

FIGURE 9: Controlled trypsin proteolysis of NOX5-containing membranes. Superoxide measurements of NOX5-containing membranes after a time course of limited trypsinolysis. The enzymatic activity was measured in the absence of Ca^{2+} and compared to the activity of a control experiment in the presence of Ca^{2+} (left). The protease-induced activity is maximal at 10 min. DPI was used as control as previously shown (*15*).

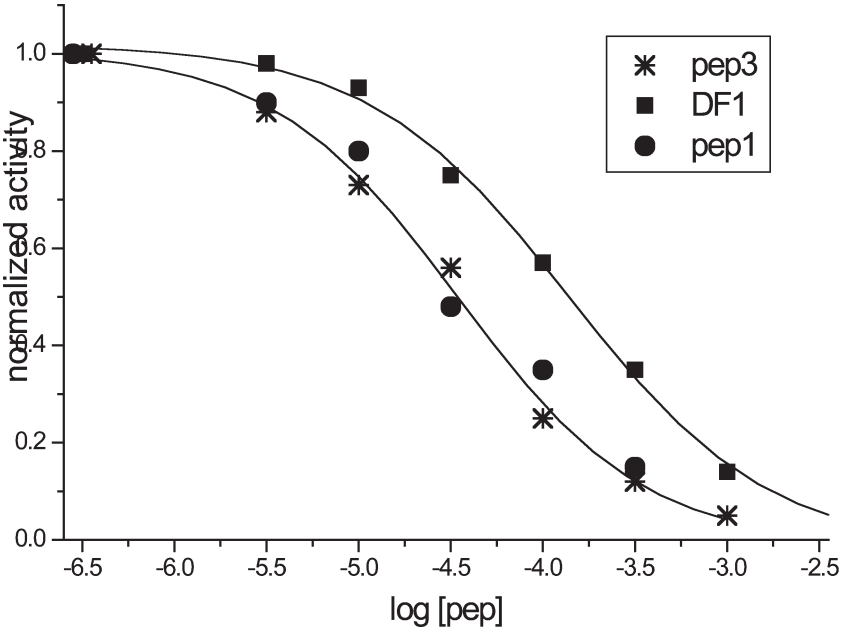

FIGURE 8: Inhibition of NOX5 activity by pep1, pep3, and DF1. Dose−response of enzymatic activity of membrane preparations from NOX5-transfected HEK293 cells in the presence of pep1 (●), pep3 (*), and DF1 (■), measured with chemiluminescense assay. Data were normalized between the minimal and maximal activity.

trypsinolysis NOX5-containing membranes do not produce superoxide in the absence of Ca^{2+}. But after 5 min of trypsin digestion, NOX5 started to generate superoxide in the absence of Ca^{2+} and reached a maximal activation of up to 75% (at 10 min in Figure 9) of the one measured with nonproteolyzed membranes in the presence of Ca^{2+} (left bar). So, after trypsinolysis the enzymatic activity becomes independent from Ca^{2+} and therefore from its N-terminal EF-hand domain, strongly suggesting that the REFBD in the catalytic domain of NOX5 has an autoinhibitory role.

DISCUSSION

The NADPH oxidase 5 is a member of the NOX family that is specialized in superoxide production (reviewed in refs *3*, *33*, and *34*). At its N-terminal end it possesses four functional EF-hand motifs (*22*), and its activation is Ca^{2+}-dependent (*12*). Previously, we have shown that upon Ca^{2+} binding the regulatory N-terminal domain undergoes a marked conformational change allowing the interaction with the catalytic C-terminal domain and thus leading to the activation of the enzyme (*22*). We have also shown that CaM binds specifically to the C-terminus of NOX5 (CaMBD) in a Ca^{2+}-dependent manner and increases the Ca^{2+} sensitivity of the enzymatic activity via the N-terminal domain (*15*).

The aim of this study was the identification of the binding site for NOX5-EF in the catalytic dehydrogenase domain (CDHD). First, we have examined a segment in the phosphorylatable region (PhosR) of NOX5 since this phosphorylation increases the Ca^{2+} sensitivity of the enzyme as shown in ref *14*. Therefore, this PhosR should be in close proximity to NOX5-EF, the sole Ca^{2+}-sensing element in the enzyme. Indeed, we found that this 17-residue peptide interacts with NOX5-EF in a Ca^{2+}-dependent manner and the interaction encompasses conformational changes. But the affinity is very weak with a K_d about 25 μM, and the conformational changes are small. These binding properties thus strongly suggest that another region in CDHD is (also) implicated in the interaction. We concentrated on the region between the PhosR and CaMBD. This is a very large region (from R496 to G661), and although we can exclude the NADPH- and FAD-binding subregions, which are identical in all NOXs, we first needed more detailed information. Cloning of rather large fragments in the region R496−G661 helped us to localize the REFBD somewhere in the region S605−T660. To narrow down the wanted site, we were inspired by the three-dimensional structure of the CDHD of NOX2 modeled on the basis of ferrodoxin−NADP reductase; Taylor and collaborators have pointed toward an α-helical insert (boxed in Table 2A) as the regulated element in NOX2 (*26*). In the sequence alignments of all the members of the NOX family we have observed that this region is well conserved in NOX1, NOX2, and NOX3 but not in NOX4 and NOX5. In addition, in NOX5 this segment is longer and completely different from all other human NOXes. It extends from D637 to T660, just before the third subregion implicated in NADPH binding (Figure 1), and it is predicted to be α-helical. Based on this information synthetic peptides were obtained, and we finally identified in the C-terminal catalytic domain CDHD a 24 amino acid long segment (REFBD) that interacts in a Ca^{2+}-dependent way with the regulatory N-terminal domain of NOX5 and displays a micromolar K_d. Their interaction provokes moderate, but distinct conformational changes as monitored by Trp (Figure 5) and TNS (not shown) fluorescence changes. At present it is not fully clear if the NOX5-EF binding site in CDHD is a single site composed of both the higher affinity REFBD and the lower affinity PhosR or if NOX5-EF alternatively interacts with each of these domains.

The K_d between the REFBD and the CDHD is about 1 μM, a quite low affinity compared to the CaM systems. But, since the two domains are located on the same polypetide chain, their interaction is intramolecular and should be entropically favored. Moreover, it is now generally accepted that, on the basis of colocalization of molecules in cell compartments, the local concentrations (*35*) are much higher (100−1000-fold), thus favoring complex formation in these confined compartments. Moreover, since the PhosR plays a role in NOX5 activation, this region *and* the REFBD may both be implicated in the interaction. The existence of a composite binding site would necessarily increase the affinity for NOX5-EF through the principle of synergism. In this respect it is notable that both pep1 and DF1, corresponding to the REFBD and the PhosR, respectively, strongly inhibit the superoxide production. The amounts to reach 90% of inhibition are high, but this again may be an effect of submembrane compartmentation. It is anticipated that linking of the two regions stabilizes them, and this may increase the binding affinity to NOX5-EF. This mechanism was already shown in the case of the complex between CaBP1 and the IP3 receptor, which regulates channel gating (*36*). The affinities of CaBP1 for the isolated N-terminal inhibitory segment and the IP3-binding domain, respectively, are very low, but CaBP1 binding increases strongly when the two are linked together. Another resembling example is the interaction S100A6 with the C-terminal domain of Siah-1 interacting protein (*21*). To answer the question of two-site binding of NOX5-EF, one could examine if it can still bind to recombinant CDHD that lacks REFBD and *vice versa*. Another obvious approach to ascertain that pep1 is a major structural element in the REFBD is to make point mutations in the NOX enzyme, express the mutants in HEK293 cells, and monitor the enzymatic activity. Carefully screening the constitutive activity and its Ca^{2+} dependency may also yield clues as to the autoinhibitory nature of the REFBD (see below). Major focus should be placed on the KKDSIT sequence, which may constitute the nucleus of the interaction.

The thermodynamic reason of the low affinity is the low negative enthalpy change (−2 kcal/mol) and very moderate entropy increase. It should be noted that the interaction of CaM with different peptides originating from target proteins is accompanied by enthalpy changes ranging from −12.6 kcal/mol (CaM kinase I) to +16 kcal/mol (melittin) (*37*). The caldesmon peptide, which interacts with CaM with an affinity comparable to that of NOX5-EF/pep1, is much more enthalpy driven (−12 kcal/mol). In contrast, the low-affinity binding of CaM to the CaM kinase II is entirely entropy driven with a ΔH of +5 kcal/mol (*38*). These data suggest that the mode of interaction of the regulatory NOX5-EF domain with the catalytic domain is different from the CaM−target interaction. In this respect it is worthwile to notice that all of the REFBD in Table 2B contain a particular motif with hydrophobic residues in positions 1 (M), 4 (I), 8 (M), and 12 (L) which may resemble the well-known motif 1, 5, 8, and 12 for CaM-binding motifs (*39*). But the positions are *not identical*, and the quality of these hydrophobic residues is quite divergent, especially in position 1 (W versus M).

The D637−T660 REFBD is unique to NOX5, where it is very well conserved in human, dog, bovine, opossum, and zebra fish (Table 2B). In insect, annelid, and mollusk NOX5 the REFBD shows nine differences in amino acid residues with human NOX5,

but internally they show more resemblance. This parallels the sequence conservation of the four EF-hands in NOX5, which are very well conserved in vertebrates but much more divergent in the invertebrate group. It is noticeable that the CaMBD and the REFBD are very different. Aromatic amino acids, especially important for CaM interaction in the CaMBD, are completely absent in the REFBD; the REFBD is more hydrophobic, and it presents an equal number of negatively and positively charged amino acids, while the CaMBD is positively charged.

In our previous study we have shown that CaM acts as a modulator of the enzymatic activity by facilitating or stabilizing the interaction between the regulatory N-terminal EF-hand domain and the catalytic C-terminal domain of NOX5. Indeed, this CaMBD is located just after the third NADPH-binding subregion whereas the REFBD identified here just precedes the third NADPH-binding subregion. Thus in space the CAMBD and the REFBD must be very close to each other. This may explain why CaM is not an independent activator with its own mechanism but acts via the NOX5-EF/REFBD activating machinery.

In addition, we have shown that the REFBD is an autoinhibitory element: after binding of Ca^{2+} to the regulatory N-terminus, the latter interacts with the REFBD and removes it from the catalytic site, thus releasing the autoinhibition of the enzyme. This mechanism is well represented by CaM and its target calcineurin phosphatase, where Ca^{2+}-CaM by interacting with its target in a well-defined region on the CaMBD releases the autoinhibition, leading to phosphatase activity (*40*, *41*). Our proposal that REFBD is an autoinhibitory domain is still based on preliminary data and must be strengthened by experiments, which delineate the trypsin cleavage site(s). But membranes of HEK293 cells likely contain too many other proteins, which will render the identification of the specific NOX5 cleavage products by mass spectrometry tantalizingly complex. An alternative elegant approach will consist of site-directed mutagenesis, especially in the KKDSIT segment of REFBD.

In summary, we demonstrated that the regulatory NOX5-EF interacts with the catalytic CDHD in two well-characterized regions, the REFBD and the PhosR. The key element for the activation is the release of the autoinhibition via the interaction of NOX5-EF with the REFBD.[2]

ACKNOWLEDGMENT

We thank Pr. Karl-Heinz Krause for allowing us to use his materials for the enzymatic activity and for advice during this project. We also thank Dr. David Fulton, who very kindly provided us with peptides and for careful reading of the manuscript, and Dr. W. R. Taylor, who provided access to the PDB file of ferrodoxin reductase-modellized NOX2.

REFERENCES

1. Lambeth, J. D. (2002) Nox/Duox family of nicotinamide adenine dinucleotide (phosphate) oxidases. *Curr. Opin. Hematol. 9*, 11–17.
2. Lambeth, J. D. (2004) NOX enzymes and the biology of reactive oxygen. *Nat. Rev. Immunol. 4*, 181–189.
3. Bedard, K., and Krause, K. H. (2007) The NOX family of ROS-generating NADPH oxidases: physiology and pathophysiology. *Physiol. Rev. 87*, 245–313.
4. Krause, K. H. (2004) Tissue distribution and putative physiological function of NOX family NADPH oxidases. *Jpn. J. Infect. Dis. 57*, S28–29.
5. Kawahara, T., and Lambeth, J. D. (2008) Phosphatidylinositol (4,5)-bisphosphate modulates Nox5 localization via an N-terminal polybasic region. *Mol. Biol. Cell 19*, 4020–4031.
6. Fulton, D. J. (2009) Nox5 and the regulation of cellular function. *Antioxid. Redox Signaling 11*, 2443–2452.
7. El Jamali, A., Valente, A. J., Lechleiter, J. D., Gamez, M. J., Pearson, D. W., Nauseef, W. M., and Clark, R. A. (2008) Novel redox-dependent regulation of NOX5 by the tyrosine kinase c-Abl. *Free Radical Biol. Med. 44*, 868–881.
8. Brar, S. S., Corbin, Z., Kennedy, T. P., Hemendinger, R., Thornton, L., Bommarius, B., Arnold, R. S., Whorton, A. R., Sturrock, A. B., Huecksteadt, T. P., Quinn, M. T., Krenitsky, K., Ardie, K. G., Lambeth, J. D., and Hoidal, J. R. (2003) NOX5 NAD(P)H oxidase regulates growth and apoptosis in DU 145 prostate cancer cells. *Am. J. Physiol. Cell Physiol. 285*, C353–C369.
9. Kamiguti, A. S., Serrander, L., Lin, K., Harris, R. J., Cawley, J. C., Allsup, D. J., Slupsky, J. R., Krause, K. H., and Zuzel, M. (2005) Expression and activity of NOX5 in the circulating malignant B cells of hairy cell leukemia. *J. Immunol. 175*, 8424–8430.
10. Desmond, B., Jay, C. A. P., Seidel-Rogol, B., Dikalova, E., Lasséguea, B., and Griendling, K. K. (2008) Nox5 mediates PDGF-induced proliferation in human aortic smooth muscle cells. *Free Radical Biol. Med. 45*, 329–335.
11. Guzik, T. J., Chen, W., Gongora, M. C., Guzik, B., Lob, H. E., Mangalat, D., Hoch, N., Dikalov, S., Rudzinski, P., Kapelak, B., Sadowski, J., and Harrison, D. G. (2008) Calcium-dependent NOX5 nicotinamide adenine dinucleotide phosphate oxidase contributes to vascular oxidative stress in human coronary artery disease. *J. Am. Coll. Cardiol. 52*, 1803–1809.
12. Banfi, B., Molnar, G., Maturana, A., Steger, K., Hegedus, B., Demaurex, N., and Krause, K. H. (2001) A Ca(2+)-activated NADPH oxidase in testis, spleen, and lymph nodes. *J. Biol. Chem. 276*, 37594–37601.
13. Spat, A. (2006) Calcium microdomains and the fine control of cell function: an introduction. *Cell Calcium 40*, 403–404.
14. Jagnandan, D., Church, J. E., Banfi, B., Stuehr, D. J., Marrero, M. B., and Fulton, D. J. (2007) Novel mechanism of activation of NADPH oxidase 5: calcium sensitization via phosphorylation. *J. Biol. Chem. 282*, 6494–6507.
15. Tirone, F., and Cox, J. A. (2007) NADPH oxidase 5 (NOX5) interacts with and is regulated by calmodulin. *FEBS Lett. 581*, 1202–1208.
16. Moldoveanu, T., Jia, Z., and Davies, P. L. (2004) Calpain activation by cooperative Ca^{2+} binding at two non-EF-hand sites. *J. Biol. Chem. 279*, 6106–6114.
17. Hoeflich, K. P., and Ikura, M. (2002) Calmodulin in action: diversity in target recognition and activation mechanisms. *Cell 108*, 739–742.
18. Crivici, A., and Ikura, M. (1995) Molecular and structural basis of target recognition by calmodulin. *Annu. Rev. Biophys. Biomol. Struct. 24*, 85–116.
19. O'Neil, K. T., and DeGrado, W. F. (1990) How calmodulin binds its targets: sequence independent recognition of amphiphilic alpha-helices. *Trends Biochem. Sci. 15*, 59–64.
20. Yap, K. L., Yuan, T., Mal, T. K., Vogel, H. J., and Ikura, M. (2003) Structural basis for simultaneous binding of two carboxy-terminal peptides of plant glutamate decarboxylase to calmodulin. *J. Mol. Biol. 328*, 193–204.
21. Lee, Y. T., Dimitrova, Y. N., Schneider, G., Ridenour, W. B., Bhattacharya, S., Soss, S. E., Caprioli, R. M., Filipek, A., and Chazin, W. J. (2008) Structure of the S100A6 complex with a fragment from the C-terminal domain of Siah-1 interacting protein: a novel mode for S100 protein target recognition. *Biochemistry 47*, 10921–10932.
22. Banfi, B., Tirone, F., Durussel, I., Knisz, J., Moskwa, P., Molnar, G. Z., Krause, K. H., and Cox, J. A. (2004) Mechanism of Ca^{2+} activation of the NADPH oxidase 5 (NOX5). *J. Biol. Chem. 279*, 18583–18591.
23. Durussel, I., Blouquit, Y., Middendorp, S., Craescu, C. T., and Cox, J. A. (2000) Cation- and peptide-binding properties of human centrin 2. *FEBS Lett. 472*, 208–212.
24. Cox, J. A., Tirone, F., Durussel, I., Firanescu, C., Blouquit, Y., Duchambon, P., and Craescu, C. T. (2005) Calcium and magnesium

[2]We tried to confirm our model in a cell-based experiment by making a mutant NOX5 lacking the region corresponding to pep1. The plasmid construction was kindly provided by Pr. Joachim Frey and expressed in HEK293T cells. Unfortunately and contrary to cells expressing the wild-type enzyme, cells expressing the mutated protein did not produce superoxide, neither in the presence nor in the absence of Ca^{2+}, likely due to a bad folding of the truncated NOX5 which impairs the transfer of the e^- via the NADPH site.

binding to human centrin 3 and interaction with target peptides. *Biochemistry 44*, 840–850.
25. Cox, J. A., Milos, M., and MacManus, J. P. (1990) Calcium- and magnesium-binding properties of oncomodulin. Direct binding studies and microcalorimetry. *J. Biol. Chem. 265*, 6633–6637.
26. Taylor, W. R., Jones, D. T., and Segal, A. W. (1993) A structural model for the nucleotide binding domains of the flavocytochrome b-245 beta-chain. *Protein Sci. 2*, 1675–1685.
27. Shatwell, K. P., Dancis, A., Cross, A. R., Klausner, R. D., and Segal, A. W. (1996) The FRE1 ferric reductase of *Saccharomyces cerevisiae* is a cytochrome *b* similar to that of NADPH oxidase. *J. Biol. Chem. 271*, 14240–14244.
28. Karplus, P. A., Daniels, M. J., and Herriott, J. R. (1991) Atomic structure of ferredoxin-$NADP^+$ reductase: prototype for a structurally novel flavoenzyme family. *Science 251*, 60–66.
29. Graf, E., Verma, A. K., Gorski, J. P., Lopaschuk, G., Niggli, V., Zurini, M., Carafoli, E., and Penniston, J. T. (1982) Molecular properties of calcium-pumping ATPase from human erythrocytes. *Biochemistry 21*, 4511–4516.
30. Tucker, M. M., Robinson, J. B., Jr., and Stellwagen, E. (1981) The effect of proteolysis on the calmodulin activation of cyclic nucleotide phosphodiesterase. *J. Biol. Chem. 256*, 9051–9058.
31. Cohen, P. (1980) The role of calcium ions, calmodulin and troponin in the regulation of phosphorylase kinase from rabbit skeletal muscle. *Eur. J. Biochem. 111*, 563–574.
32. Singh, T. J., and Wang, J. H. (1979) Stimulation of glycogen phosphorylase kinase from rabbit skeletal muscle by organic solvents. *J. Biol. Chem. 254*, 8466–8472.
33. Lambeth, J. D., Kawahara, T., and Diebold, B. (2007) Regulation of Nox and Duox enzymatic activity and expression. *Free Radical Biol. Med. 43*, 319–331.
34. Vignais, P. V. (2002) The superoxide-generating NADPH oxidase: structural aspects and activation mechanism. *Cell. Mol. Life Sci. 59*, 1428–1459.
35. Kuriyan, J., and Eisenberg, D. (2007) The origin of protein interactions and allostery in colocalization. *Nature 450*, 983–990.
36. Li, C., Chan, J., Haeseleer, F., Mikoshiba, K., Palczewski, K., Ikura, M., and Ames, J. B. (2009) Structural Insights into Ca^{2+}-dependent regulation of inositol 1,4,5-trisphosphate receptors by CaBP1. *J. Biol. Chem. 284*, 2472–2481.
37. Brokx, R. D., Lopez, M. M., Vogel, H. J., and Makhatadze, G. I. (2001) Energetics of target peptide binding by calmodulin reveals different modes of binding. *J. Biol. Chem. 276*, 14083–14091.
38. Tse, J. K., Giannetti, A. M., and Bradshaw, J. M. (2007) Thermodynamics of calmodulin trapping by Ca^{2+}/calmodulin-dependent protein kinase II: subpicomolar K_d determined using competition titration calorimetry. *Biochemistry 46*, 4017–4027.
39. Yap, K. L., Kim, J., Truong, K., Sherman, M., Yuan, T., and Ikura, M. (2000) Calmodulin target database. *J. Struct. Funct. Genomics 1*, 8–14.
40. Hubbard, M. J., and Klee, C. B. (1989) Characterization of a high-affinity monoclonal antibody to calcineurin whose epitope defines a new structural domain of calcineurin A. *Eur. J. Biochem. 185*, 411–418.
41. Perrino, B. A. (1999) Regulation of calcineurin phosphatase activity by its autoinhibitory domain. *Arch. Biochem. Biophys. 372*, 159–165.